

^{13}C – ^{13}C Correlation Spectroscopy of Membrane-Associated Influenza Virus Fusion Peptide Strongly Supports a Helix-Turn-Helix Motif and Two Turn Conformations

Yan Sun and David P. Weliky*

Department of Chemistry, Michigan State University, East Lansing, Michigan 48824

Received June 24, 2009; E-mail: weliky@chemistry.msu.edu

Enveloped viruses such as influenza virus are surrounded by a membrane, and infection of target cells begins with joining or “fusion” of viral and host cell membranes into a single membrane.¹ Although membrane fusion is thermodynamically allowed, there is a high kinetic barrier to the fusion process. For this reason, enveloped viruses contain “fusion protein” which catalyzes membrane fusion. For influenza virus, hemagglutinin (HA) is the fusion protein and consists of HA1 and HA2 subunits. The ~20 residues of the HA2 N-terminus are known as the influenza fusion peptide (IFP) and play a critical role in fusion. IFP is initially buried within HA while the influenza virus is endocytosed into the target cell. The low pH of the endosome (~5) triggers a conformational change of HA, and the IFP is exposed and binds to the endosomal membrane with consequent fusion between the viral and endosomal membranes. This paper focuses on the IFP in the absence of the remaining fusion protein. The peptide with IFP sequence serves as a good model system to understand the role of the IFP in influenza viral fusion as evidenced by IFP-induced lipid vesicle fusion at low pH and by the strong correlation between mutation–activity relationships of IFP-induced vesicle fusion and HA-catalyzed cell membrane fusion.² IFP is also an important system for developing and testing different simulation methods for membrane-associated peptides.^{3–7} It is therefore necessary to have high-resolution structural information for the membrane-associated IFP.

Structures of detergent-associated IFP have been determined by liquid-state NMR and, at pH 5.0, showed an N-terminal helix from residues 2–10 followed by a turn followed by a C-terminal helix from residues 13–18 and, at pH 7.4, showed an N-terminal helix from residues 2–9 followed by a turn and C-terminal extended structure.⁸ In membranes, there is substantial experimental support for the N-terminal helical structure and much less support for the turn and C-terminal structure.^{2,8–10} Molecular dynamics simulations on membrane-associated IFP from different groups have had conflicting results with observation of helix-turn-helix structure as well as continuous helical structure without a turn.^{5–7} In the present work, the conformation of the putative turn region in membrane-associated IFP has been probed with solid-state NMR spectroscopy. The significance of this study is highlighted by observation of IFP-induced fusion between membrane vesicles but not between detergent micelles.

IFP has the sequence GLFGAIAGFIENGWEGMIDGGGKKK-KG where the underlined residues represent the HA2 N-terminus and the subsequent residues increase aqueous solubility. IFP-I10E11 was U- ^{13}C , ^{15}N labeled at Ile-10 and Glu-11 and IFP-N12G13 was U- ^{13}C , ^{15}N labeled at Asn-12 and Gly-13. Additional IFPs were synthesized with a single ^{13}CO label or a single ^{13}CO and a single ^{15}N label and are described in the Supporting Information (SI). The solid-state NMR samples contained 0.8 μmol of IFP, 16 μmol of DTPC lipid, and 4 μmol of DTPG lipid and were hydrated with

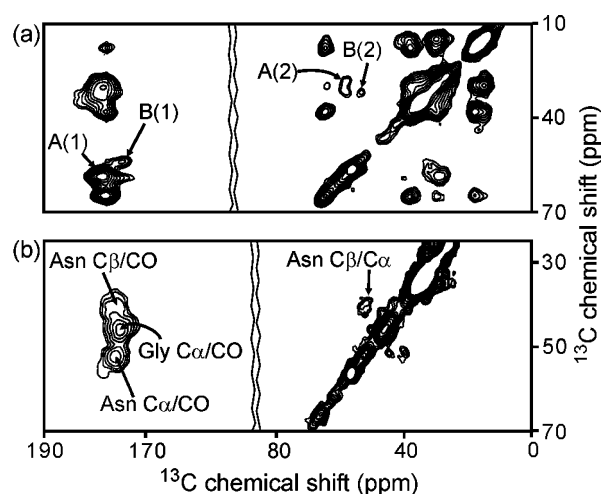


Figure 1. NMR spectra of membrane-associated (a) IFP-I10E11 and (b) IFP-N12G13 at pH 5.0. Some of the peak assignments are shown using the convention f_1 (vertical axis)/ f_2 (horizontal axis). The A and B labels represent two distinct sets of Glu-11 crosspeaks: A(1) and B(1), Glu-11 C α /CO; A(2) and B(2), Glu-11 C β /C α .

buffer. ^{13}C – ^{13}C correlation spectra were generated with proton-driven spin diffusion (PDS) using 10 ms of exchange which led to observation of only intraresidue crosspeaks.⁹

Figure 1 displays PDS spectra of membrane-associated IFP-I10E11 and IFP-N12G13 at fusogenic pH 5.0. The peaks were assigned based on the characteristic chemical shifts of the amino acid spin systems, and Table 1 lists the ^{13}C shifts. Two distinct sets of crosspeaks were observed for Glu-11, and the ratio of intensities of the two peak sets A/B is ~3:1. Backbone dihedral angles were derived from a TALOS program-based analysis of the ^{13}C chemical shifts obtained from the Figure 1 spectra and from spectra of membrane-associated IFP which was either singly ^{13}CO labeled or U- ^{13}C , ^{15}N labeled from residues 1 through 10.^{9,11} The Ile-10 to Gly-13 angles are listed in Table 1, and the Gly-1 to Phe-9

Table 1. ^{13}C Chemical Shifts in ppm and Dihedral Angles in degrees for IFP-I10E11 and IFP-N12G13 Samples at pH 5.0

	CO	C α	C β	C γ	C δ	$\varphi/\psi^{c,d}$	$\varphi/\psi^{d,e}$
I10	178.0	65.1	38.2	30.0, 17.9 ^a	15.2	-64/-42	-70/-34
E11	A	178.7	58.8	28.9	37.2	181.9 ^b	-69/-26
	B	174.5	54.0	32.0	37.9		-126/156
N12	175.5	51.4	39.8	175.0		-96/8	-113/125
G13	174.5	45.8				87/10	87/10

^a γ -CH₂ and γ -CH₃, respectively. ^b Chemical shift of COO⁻. ^c Dihedral angles corresponding to shift set A of E11. ^d The average uncertainty is $\pm 13^\circ$, and specific uncertainties are given in the SI based on distributions of TALOS results. ^e Dihedral angles corresponding to shift set B of E11.

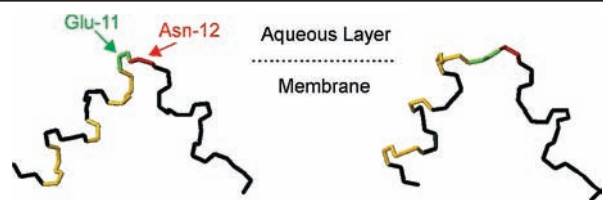


Figure 2. Backbone structures of membrane-associated IFP based on (left) Glu-11 shift set A or (right) Glu-11 shift set B. Glu-11 is in green, Asn-12 is in red, and the hydrophobic residues Leu-2, Phe-3, Ile-6, Phe-9, and Ile-10 are in gold. The structures are drawn from the perspective of “inverted V” membrane insertion with the membrane normal along the symmetry axis of the V and the lipid/water interface near Glu-11 and Asn-12. An alternate view is shown in the SI.

angles are provided in the SI. Figure 2 displays two backbone structures based on these angles and correlated with the A and B crosspeaks in Figure 1. The Trp-14 to Gly-20 dihedral angles in both structures were obtained from the pH 5.0 IFP structures in detergent micelles and were supported by the solid-state NMR observation of helical structure in this region of membrane-associated IFP at both pH 5.0 and pH 7.4; cf. SI.⁸ In both the A and B structures, the membrane-associated IFP adopts a helix-turn-helix conformation. Detection of two distinct turn conformations at pH 5.0 is supported by (1) Glu-11 A and B shifts which respectively correlate with canonical shifts of helical and β strand conformations; (2) Asn-12 shifts that do not correlate with helical conformation; (3) solid-state NMR measurement of a 3.6 Å Phe-9 ¹³CO-Gly-13 ¹⁵N distance that agrees quantitatively with the distance in the A structure (cf. SI); and (4) interpretation of ESR spectra of spin-labeled IFP.^{12,13} The B crosspeaks are only present for samples at more fusogenic lower pH and are absent for samples at less fusogenic pH 7.4, Figure 3. At pH 7.4, the A/B population ratio is ≥ 10 as estimated from the signal-to-noise of the A crosspeaks. The B conformation may not have been observed in detergent structures because of rapid motional averaging between the A and B structures. The B structure may be correlated with increased fusion at pH 5.0 through the hypothesized “inverted V” insertion of IFP into the membrane, Figure 2.⁸ Consider the reasonable hypothesis that the fusion rate is correlated with membrane insertion of the IFP and the resulting membrane perturbation. Membrane insertion would be favored for the pH 5.0 B structure because of the placement of the N-terminal hydrophobic residues on the outside of the V shape in contact with the hydrophobic region of the membrane. In addition to functional relevance, observation of two distinct local conformations in a small membrane-associated peptide is of fundamental interest and the structures provide important data for development of simulation methods that can in principle detect the full IFP conformational distribution.^{6,7}

Glu-11, for which two shift sets were observed, is critical for HA2-mediated fusion and for the pH dependence of IFP-mediated vesicle fusion.^{14,15} The protonation state of the side chain of Glu-11 was probed as a function of pH through its C δ shift and relied on the downfield shift of COO⁻ relative to COOH, Figure 3. The Glu-11 C γ /C δ (COO⁻) crosspeak was absent at pH 4.0, became apparent at pH 5.0, and was strong at pH 7.4. Increasing pH also showed a concurrent decrease in intensity in the region containing the C γ /C δ (COOH) crosspeak. This pH dependence in membranes correlates with the Glu-11 pK_a of 5.9 in detergent and suggests that the Glu-11 side chain has contact with water which is consistent with the inverted V membrane location model.¹⁶ The structures in Figure 2 suggest a connection between Glu-11 side chain protonation and formation of the B structure: the charged Glu-11 COO⁻

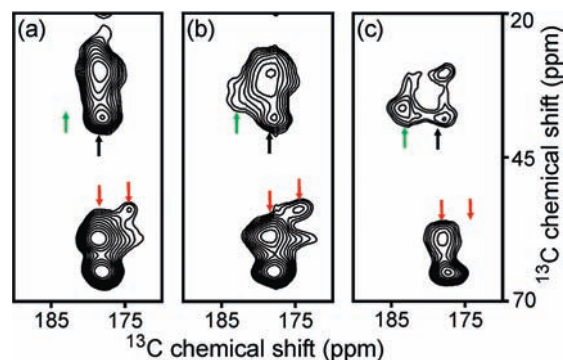


Figure 3. NMR spectra of membrane-associated IFP-UI10E11 at (a) pH 4.0; (b) pH 5.0; and (c) pH 7.4. Green arrows point to the Glu C γ /C δ (COO⁻) crosspeak. This crosspeak is absent at pH 4.0. Black arrows point to the Glu C γ /C δ (COOH) crosspeak which is overlapped with other crosspeaks. Red arrows point to crosspeaks of Glu C α /CO A (left) and B (right). The B crosspeak is absent at pH 7.4.

side chain in the A structure points toward the aqueous layer, whereas the uncharged COOH in the B structures points toward the membrane interior. The protonation information from Figure 3 will be useful for molecular dynamics studies of the membrane-associated IFP for which protonation states are input parameters.⁶

In summary, solid-state NMR spectra strongly support a helix-turn-helix motif for the membrane-associated IFP at both more fusogenic pH 5.0 and less fusogenic pH 7.4 and a second turn conformation at pH 5.0 which correlates with protonation of the Glu-11 side chain. The NMR results provide insight into the pH dependence of IFP fusion activity and are overall consistent with inverted V membrane location of IFP. The IFP is an important system for testing simulation methods for membrane-associated peptides, and the NMR structures provide significant constraints for this method development.

Acknowledgment. This work was supported by NIH Award AI47153.

Supporting Information Available: Descriptions of experiments and additional experimental data and analysis. This information is available free of charge via the Internet at <http://pubs.acs.org>.

References

- (1) White, J. M.; Delos, S. E.; Brecher, M.; Schornberg, K. *Crit. Rev. Biochem. Mol. Biol.* **2008**, *43*, 189–219.
- (2) Nieva, J. L.; Agirre, A. *Biochim. Biophys. Acta* **2003**, *1614*, 104–115.
- (3) Huang, Q.; Chen, C. L.; Herrmann, A. *Biophys. J.* **2004**, *87*, 14–22.
- (4) Vaccaro, L.; Cross, K. J.; Kleinjung, J.; Straus, S. K.; Thomas, D. J.; Wharton, S. A.; Skehel, J. J.; Fraternali, F. *Biophys. J.* **2005**, *88*, 25–36.
- (5) Lague, P.; Roux, B.; Pastor, R. W. *J. Mol. Biol.* **2005**, *354*, 1129–1141.
- (6) Sammalkorpi, M.; Lazaridis, T. *Biochim. Biophys. Acta* **2007**, *1768*, 30–38.
- (7) Jang, H.; Michaud-Agrawal, N.; Johnston, J. M.; Woolf, T. B. *Proteins: Struct., Funct., Bioinform.* **2008**, *72*, 299–312.
- (8) Han, X.; Bushweller, J. H.; Cafiso, D. S.; Tamm, L. K. *Nat. Struct. Biol.* **2001**, *8*, 715–720.
- (9) Bodner, M. L.; Gabrys, C. M.; Struppe, J. O.; Weliky, D. P. *J. Chem. Phys.* **2008**, *128*, 052319.
- (10) Macosko, J. C.; Kim, C. H.; Shin, Y. K. *J. Mol. Biol.* **1997**, *267*, 1139–1148.
- (11) Cornilescu, G.; Delaglio, F.; Bax, A. *J. Biomol. NMR* **1999**, *13*, 289–302.
- (12) Zhang, H. Y.; Neal, S.; Wishart, D. S. *J. Biomol. NMR* **2003**, *25*, 173–195.
- (13) Lai, A. L.; Tamm, L. K. *J. Biol. Chem.* **2007**, *282*, 23946–23956.
- (14) Korte, T.; Eband, R. F.; Eband, R. M.; Blumenthal, R. *Virology* **2001**, *289*, 353–361.
- (15) Lai, A. L.; Park, H.; White, J. M.; Tamm, L. K. *J. Biol. Chem.* **2006**, *281*, 5760–5770.
- (16) Chang, D. K.; Cheng, S. F.; Lin, C. H.; Kantchev, E. A. B.; Wu, C. W. *Biochim. Biophys. Acta* **2005**, *1712*, 37–51.

JA905198Q